Static and Dynamic Dielectric Polarization and Viscosity of *n*-Hexylcyanobiphenyl in the Isotropic and Nematic Phases

Jan Jadżyn, Grzegorz Czechowski, and Danuta Bauman[a]

Institute of Molecular Physics, Polish Academy of Sciences, Smoluchowskiego 17, 60-179 Poznań, Poland
[a] Faculty of Technical Physics, Poznań University of Technology, Piotrowo 3, 60-965 Poznań, Poland

Reprint requests to Prof. J. J.; Fax (61) 86-84-524; E-mail: jadzyn@ifmpan.poznan.pl

Z. Naturforsch. **55a,** 810–816 (2000); received June 24, 2000

On the basis of the temperature dependence of the static principal permittivities, $\varepsilon_{\parallel}$ and $\varepsilon_{\perp}$, measured for the nematic phase of *n*-hexylcyanobiphenyl (C_6H_{13}–Ph–Ph–C≡N, 6CB), a value of the angle β between the long molecular axis and the direction of the dipole moment μ of 6CB, as well as the order parameter $S(T)$, were obtained by use of the Maier-Meier equations. From the dielectric relaxation and viscosity data, the contribution of the nematic potential to the molecular dynamics was estimated. In the isotropic phase the dielectric and viscosity data allow one, in the framework of the Debye model, to estimate the effective length of 6CB molecule.

Key words: Electric Permittivity; Dielectric Relaxation; Viscosity; 6CB.

1. Introduction

Dielectric studies of liquids and liquid crystals provide us with useful molecular data concerning their structure, interactions and aggregation processes. The most propitious circumstances can be found in studies of nematic liquid crystals. The possibility of control of the molecular orientation in the whole nematic sample by an electric/magnetic field or by an appropriate preparation of the capacitor electrode surfaces, allows one to record the dielectric response on the directions of the principal molecular axes [1–3].

From analysis of the temperature dependence of the static permittivities, $\varepsilon_{\parallel}(T)$ and $\varepsilon_{\perp}(T)$, measured parallel and perpendicular to the molecular orientation (director $\boldsymbol{n}$), the angle between the resultant dipole moment of the nematogen molecule and its long axis can be obtained [4, 5]. It is a unique experimental method, which allows one to obtain this quantity in the liquid state. Simultaneously, the analysis gives reliable values of the orientational order parameter $S(T)$, which can be compared with the $S(T)$ dependences obtained with other methods.

The temperature and the frequency dependences of the permittivities afford the basic data on the dynamic of the nematogen molecules. Besides, if the viscosity data are available, the contribution of the nematic potential to the molecular dynamics and the effective length of the rotating molecule (in the isotropic phase) can be estimated from the dielectric relaxation data [6–8].

2. Experimental

n-Hexylcyanobiphenyl (6CB) was synthesized and purified at the Institute of Chemistry, Military University of Technology, Warsaw. The compound has the following sequence of phase transitions: crystal (Cr) 14.5 °C – nematic (N) 29 °C – isotropic (I).

The static electric permittivity was measured with a Wayne Kerr 6425 Precision Component Analyser at 10 kHz. The nematic sample, placed between two plane electrodes of the capacitor, was oriented with a magnetic field of about 0.6 T. The permittivities $\varepsilon_{\parallel}$ and $\varepsilon_{\perp}$ were determined for different orientations of the probing electric field $\boldsymbol{E}$ with respect to the orienting magnetic field $\boldsymbol{B}$: $\boldsymbol{E} \parallel \boldsymbol{B}$ and $\boldsymbol{E} \perp \boldsymbol{B}$, respectively.

The dielectric relaxation spectra were recorded with a HP 4194A Impedance/Gain-Phase Analyser in the frequency range of 100 kHz–100 MHz. The concentric output (via a HP 4194A impedance probe) used for the measurements up to 100 MHz requires a capacitor of a special design. The capacitor we used consists of three plane electrodes: one central ("hot") electrode and two grounded electrodes on each side. Because the impedance probe is very sensitive to the magnetic field, a biasing d.c. electric field was used for the ordering the nematic sample. Of course, in such circumstances only the dielectric spectrum $\varepsilon^*_{\parallel}(\omega)$ can be recorded.

The density was measured with an Anton Paar DMA 60/602 vibration tube densimeter. The viscosity was measured with a Haake viscometer Rotovisco RV20 with

0932-0784 / 2000 / 0900-0810 $ 06.00

a measuring system CV 100. The system consists of a rotary beaker filled with the liquid being studied and a cylindrical sensor of the Mooney-Evart type (ME15), placed in the centre of the beaker. The liquid gap was 0.5 mm.

3. Results and Discussion

Static Permittivities

Figure 1 a presents the temperature dependence of the static permittivities measured for the nematic and isotropic phases of 6CB. The results can be interpreted by use of the Maier-Meier theory [4], according to which the electric permittivities measured parallel ($\varepsilon_{\parallel}$) and perpendicular ($\varepsilon_{\perp}$) to the director $\boldsymbol{n}$ are related to the molecular quantities by the equations

$$\varepsilon_{\parallel} = 1 + \frac{N h F}{\varepsilon_0} \cdot \left\{ \bar{\alpha} + \frac{2}{3} \Delta\alpha \cdot S + F \cdot \frac{\mu_{\mathrm{app}}^2}{3kT} [1 - (1 - 3\cos^2 \beta) \cdot S] \right\}, \quad (1)$$

$$\varepsilon_{\perp} = 1 + \frac{N h F}{\varepsilon_0} \cdot \left\{ \bar{\alpha} - \frac{1}{3} \Delta\alpha \cdot S + F \cdot \frac{\mu_{\mathrm{app}}^2}{3kT} \left[1 + \frac{1}{2} (1 - 3\cos^2 \beta) \cdot S \right] \right\}, \quad (2)$$

where $\varepsilon_0 = 8.85 \cdot 10^{-12}\ \mathrm{F \cdot m^{-1}}$, N is the number of molecules per unit volume, and h and F are the Onsager local field factors:

$$h = \frac{3\bar{\varepsilon}}{2\bar{\varepsilon} + 1}, \quad F = \frac{1}{1 - \bar{\alpha} f}, \quad f = \frac{2(\bar{\varepsilon} - 1)}{2\bar{\varepsilon} + 1} \frac{N}{3\varepsilon_0}. \quad (3)$$

$\bar{\alpha}$ and $\bar{\varepsilon}$ are the mean values of the polarizability and the permittivity, respectively:

$$\bar{\alpha} = \frac{1}{3}(\alpha_{\mathrm{l}} + 2\alpha_{\mathrm{t}}), \quad \bar{\varepsilon} = \frac{1}{3}(\varepsilon_{\parallel} + 2\varepsilon_{\perp}). \quad (4)$$

$$\Delta\alpha = \alpha_{\mathrm{l}} - \alpha_{\mathrm{t}} \quad (5)$$

denotes the anisotropy of the polarizability. α_{l} and α_{t} are the components of the polarizability tensor along the long and short molecular axis, respectively. β is the angle between the total dipole moment vector $\boldsymbol{\mu}$ of the nematogenic molecule and its long axis. S is the order parameter, defined as

$$S = \frac{1}{2} \left\langle 3\cos^2 \Theta - 1 \right\rangle, \quad (6)$$

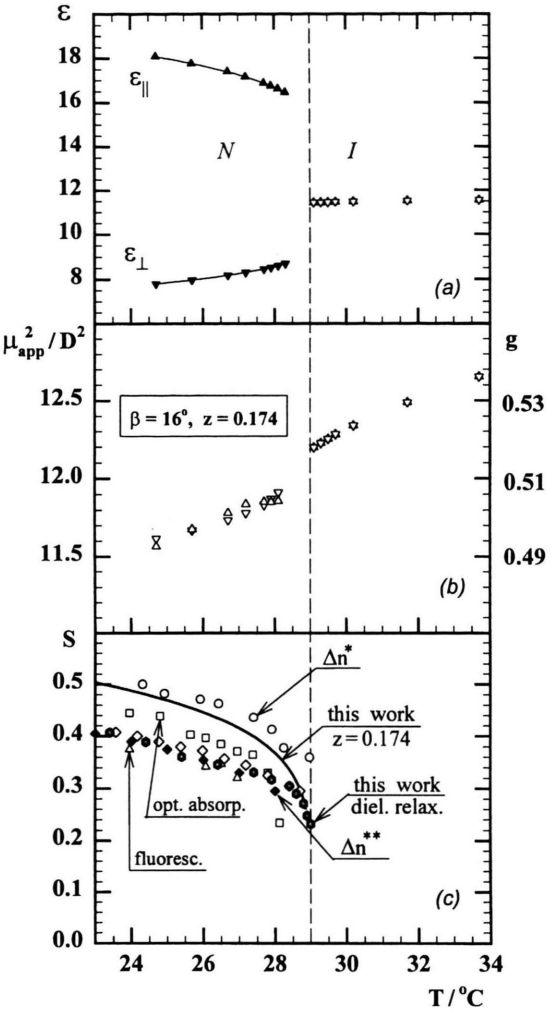

Fig. 1. (a) The solid lines present the best fitting of the Maier-Meier equations (1) and (2) to the experimental data of $\varepsilon_{\parallel}(T)$ and $\varepsilon_{\perp}(T)$ for 6CB. (b) The compliance with the requirement of the equality of μ_{app}^2 in both equations gives $\beta = 16°$ and $z = 0.174$. (c) The $S(T)$ dependence obtained in the dielectric investigations (static and dynamic) of this work is compared with that resulting from Δn^* [9], Δn^{**} [10], optical absorption [11] and fluorescence [11] measurements.

where Θ is the angle between the long molecular axis and the director $\boldsymbol{n}$.

For isotropic phase ($\varepsilon_{\parallel} = \varepsilon_{\perp} = \varepsilon$, $S = 0$), (1) and (2) transform into the Onsager equation [12]

$$\frac{(\varepsilon - \varepsilon_{\infty})(2\varepsilon + \varepsilon_{\infty})}{\varepsilon(\varepsilon_{\infty} + 2)^2} = \frac{N}{3\varepsilon_0} \frac{\mu_{\mathrm{app}}^2}{3kT}, \quad (7)$$

where ε_{∞} denotes high frequency value of the permittivity (often taken as the refraction index n). ε_{∞} and the pola-

rizability α are connected by the equation

$$\frac{\varepsilon_\infty - 1}{\varepsilon_\infty + 2} = \frac{N}{3\varepsilon_0}\alpha . \tag{8}$$

Because the Onsager local field model does not take into account the intermolecular (dipolar) correlation, the apparent dipole moment (μ_{app}) is introduced in (1), (2), and (7). The relation between μ_{app} and the dipole moment of the isolated molecule (μ_0) is often expressed by the Kirkwood correlation factor g:

$$g = \mu_{app}^2/\mu_0^2. \tag{9}$$

The value of g indicates directly the predominant type of intermolecular interactions in the system investigated: for $g > 1$ the parallel dipolar correlations, and for $g < 1$ the antiparallel correlations.

There are three unknown quantities in (1) and (2). Two of them concern the nematogen molecule; they are (i) the angle β between the resultant dipole moment μ of the molecule and its long axis and (ii) the square of the apparent dipole moment μ_{app}^2 of the molecule. The third is the macroscopic order parameter $S(T)$. These three quantities can be obtained from the fitting of the Maier-Meier equations to the experimental data. It is commonly accepted that the $S(T)$ dependence is taken from another experiment, for example optical or magnetic anisotropy measurements. In principle, the $S(T)$ dependence can be derived from measurements of any anisotropic properties of the nematic liquid crystal [6]. However, differences of about 10% in the $S(T)$ determined by different methods are typical.

It was shown in [5] that the values of β and μ_{app}^2 resulting from the fitting are very sensible to the $S(T)$ function and even change of a few per cent in $S(T)$ give significant changes in β and $\mu_{app}^2(T)$. Often, the reproduction of the experimental data of $\varepsilon_{\parallel}(T)$ and $\varepsilon_{\perp}(T)$ by the Maier-Meier equations, with the use of the $S(T)$ dependence taken from an experiment, leads to a different $\mu_{app}^2(T)$ dependence in (1) and (2). This is obviously a non-physical result, because $\mu_{app}^2(T)$ in the two Maier-Meier equations is by definition the same. So, the fitting procedure must obey the following condition: at a given temperature, the value of μ_{app}^2 in (1) and (2) must be the same. That physical self-evident condition makes the fitting of the Maier-Meier equations to the experimental data unequivocal and, as a result, one obtains values of the three quantities β, $\mu_{app}^2(T)$ and $S(T)$. The fitting procedure becomes quite simple when the $S(T)$ dependence is expressed in the empirical formula [13]

$$S(T) = \left(1 - \frac{T}{T_{NI}}\right)^z , \tag{10}$$

where T_{NI} denotes the nematic to isotropic phase transition temperature. The temperature dependence of the nematic order parameter is then determined by one parameter (z) only.

The values of $\bar{\alpha} = 33.7 \cdot 10^{-24}$ cm^3 and $\Delta\alpha = 17.6 \cdot 10^{-24}$ cm^3 for 6CB were taken from [14].

The solid lines in Figure 1(a) represent the best fitting of the Maier-Meier equations (1) and (2) to the measured permittivities. The condition concerning μ_{app}^2 in the nematic phase is fulfilled, as can be seen in Figure 1(b). The figure displays also the value of β and z resulting from the fitting. The solid line in Figure 1(c) represents the function $S(T)$ plotted for $z = 0.174$. The $S(T)$ dependence obtained is compared with that obtained with other methods.

In the Fig. 1(b) the values of $\mu_{app}^2(T)$ are expressed in the dimensionless quantity g (9), for the dipole moment of a single 6CB molecule $\mu_0 = 4.8$ D [15]. The g-values smaller than unity indicate the antiparallel dipolar correlations. The transition from the isotropic phase to the nematic phase manifests itself by an essential increase in degree of the antiparallel dipolar association (the decrease of g) [16].

Dielectric Relaxation

Figure 2 presents the dielectric relaxation spectra recorded in the isotropic and nematic phases of 6CB. In the latter phase the permittivity was measured for $\boldsymbol{E} \| \boldsymbol{n}$. The analysis of the dielectric relaxation spectra of 6CB can be carried out by use of the molecular model presented in [8]. In the oriented nematic sample, the nematogen molecule rotates around the three axes of symmetry (see Figure 3). Two of them concern the molecule itself (the long and short molecular axes) and the third axis is the director $\boldsymbol{n}$. For a typical nematogen substance (like 6CB), the electromagnetic energy absorption due to these three modes of rotation can be expected in the frequency region from several megahertz to several gigahertz.

Because the energy absorption appears only when the molecular rotation is followed by changes of the projection of the molecular dipole moment on the direction of the measuring electric field vector $\boldsymbol{E}$, in the $\varepsilon_{\parallel}^*(\omega)$ dominates the absorption due to the molecular rotation around the short axis (Fig. 3a). Also the absorption band due to the molecular rotation around the long axis should appear in the spectrum. For a perfectly oriented nematic sample the molecular rotation on the cone around the director $\boldsymbol{n}$ (Fig. 3(b)) gives no contribution to the $\varepsilon_{\parallel}^*(\omega)$ spectrum. The band 2 dominates in the $\varepsilon_{\perp}^*(\omega)$ spectrum [8].

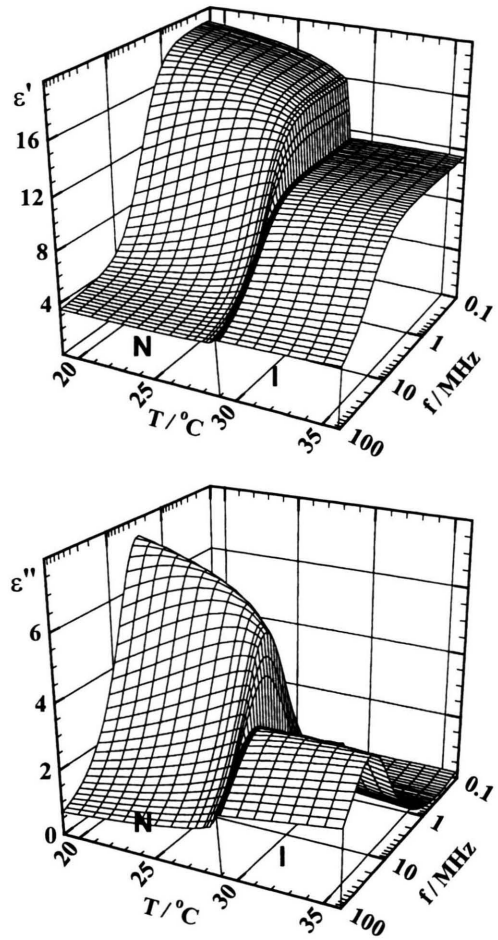

Fig. 2. Dielectric dispersion (ε') and absorption (ε'') of 6CB in the isotropic (I) and nematic (N) phases. In the nematic phase the permittivity was measured for $\boldsymbol{E}\|\boldsymbol{n}$.

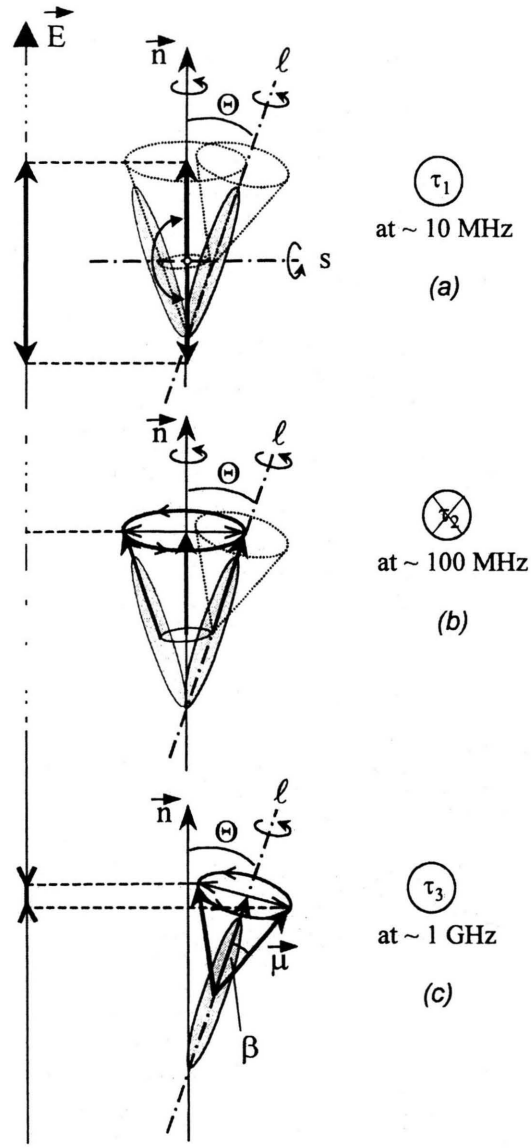

Fig. 3. For the perfectly oriented nematic with $\boldsymbol{E}\|\boldsymbol{n}$, the dielectric relaxation spectrum is composed of two absorption bands corresponding to the molecular rotation around the short (τ_1) and long (τ_3) molecular axes.

Figure 4 presents examples of the resolution of experimental spectra of 6CB in the isotropic and nematic phases into elementary contributions with use of an empirical Cole-Cole formula [17]

$$\varepsilon^*(\omega) = \varepsilon'(\omega) - j\varepsilon''(\omega) = \varepsilon_\infty + \sum_i \frac{A_i}{1 + (j\omega\tau_i)^{1-k_i}}. \tag{11}$$

The formula takes into account a distribution of relaxation times. For the limiting value of the distribution parameter $k_i = 0$, the i-th relaxation process is described by a single relaxation time (the Debye-type process). A_i and τ_i denote the dielectric strength and the relaxation time, respectively, and together with the k_i, they are the adjustable parameters in the fitting of (11) to the experimental spectrum.

The dashed lines in Fig. 4 represent the elementary spectra, which correspond to the two molecular movements observed for the orientation $\boldsymbol{E}\|\boldsymbol{n}$. As can be seen, in the studied range of frequencies only a small part of the band 3 appears in the spectrum, especially in the nemat-

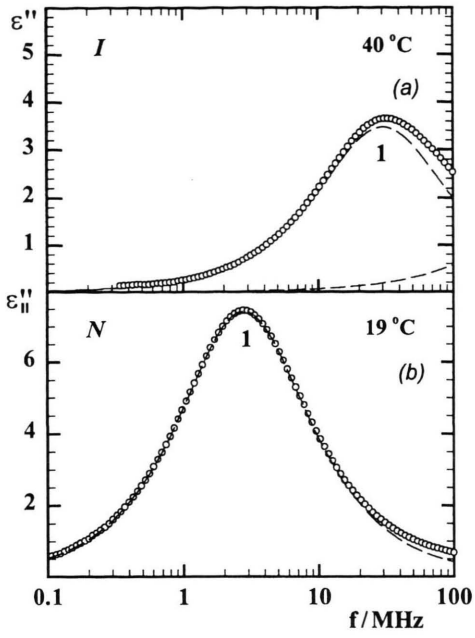

Fig. 4. Examples of the resolution of the experimental dielectric absorption spectra of 6CB recorded in the isotropic and nematic phases (points) into Debye-type contributions (dashed lines).

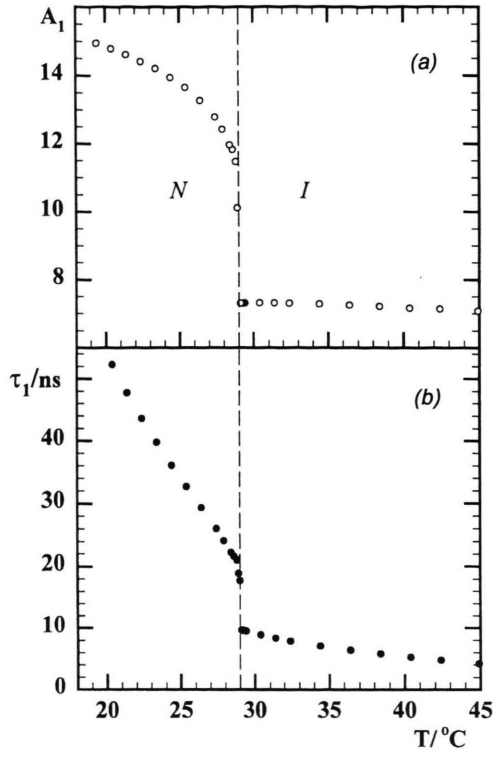

Fig. 5. (a) The dielectric strength and (b) the relaxation time corresponding to the 6CB molecule rotation around the short axis, as functions of the temperature.

ic phase. So, further on we will discuss only the band 1, i.e. we will be interested in the molecular rotation around the short axis. This type of molecular movement yields the most important information about the molecular dynamics in the presence of the nematic potential.

The values of the k_1 parameter resulting from the fitting procedure were about 10^{-2} both in the isotropic and nematic phases, i.e. band 1 is very close to the Debye-type.

The temperature dependences of the dielectric strength A_1 and the relaxation time τ_1 are presented in Figure 5. At the temperature of the phase transition from the isotropic to nematic phase one observes a jump in the values both A_1 and and τ_1. The temperature dependence of the relaxation time τ_1 can be interpreted if the viscosity of the medium is known.

Figure 6 shows the temperature dependence of the viscosity of 6CB measured in the isotropic and nematic phases. At the isotropic to nematic transition temperature a sharp decrease of the viscosity is observed. It is due to the well-known flow alignment effect occurring in the nematic phase [6]. The effect leads to the situation where the macroscopic ordering of the nematic liquid crystal becomes (roughly) parallel to the velocity v and perpendicular to the velocity gradient. Then, the nematic viscosity has the smallest possible value. In terms of Mięsowicz viscosity coefficients [18] the viscosity measured in our experiment is close to η_2.

Figure 7 presents Arrhenius plots for the relaxation time τ_1 and the viscosity in the isotropic and nematic phases of 6CB. In the isotropic phase the activation energy for the molecular rotation around the short axis and that of the viscous flow are quite close to each other. This means that in the isotropic phase of 6CB the viscosity is the main factor which determines the molecular dynamics reflected in the dielectric spectra as band 1 (Figure 4a). If so, one can try to use the Debye model [7] for the evaluation of the effective length of the 6CB molecule. In the model the rotating dipolar, rigid and axially symmetric molecule is represented by a sphere of diameter ℓ. The relation between the dielectric relaxation time, corresponding to the molecular rotation around its short axis (τ_1) and the viscosity (η) of the isotropic medium in which the sphere is moving, has the form

$$\tau_1^{\mathrm{iso}} = \frac{\pi \ell^3 \eta^{\mathrm{iso}}}{2kT}, \tag{12}$$

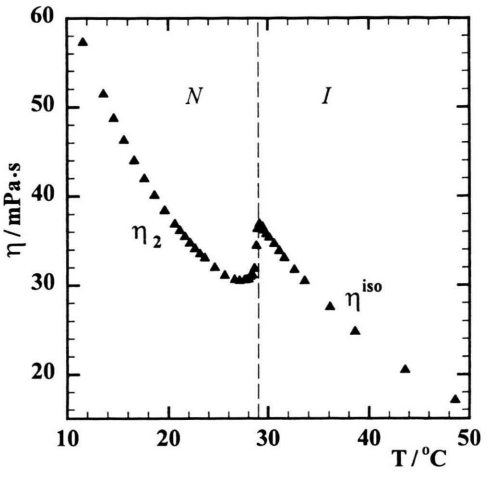

Fig. 6. The temperature dependence of the viscosity of 6CB in the isotropic and nematic phases.

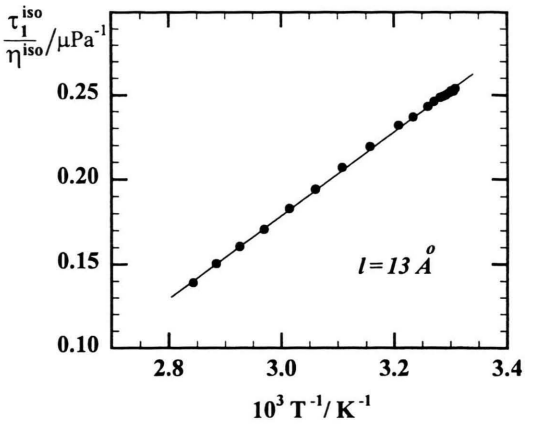

Fig. 8. Dependence of the τ_1/η on T^{-1} in the isotropic phase of 6CB resulting from the Debye model (12). ℓ denotes the apparent length of the 6CB molecule rotating around its short axis.

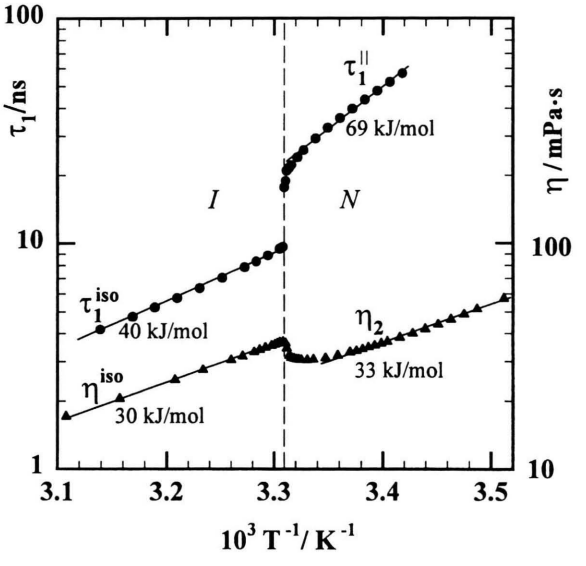

Fig. 7. Arrhenius plots for the relaxation time τ_1 and the viscosity of 6CB. The values of the activation energy are given in the figure.

where T is the absolute temperature and k the Boltzmann constant. The linear dependence of the relaxation time to viscosity ratio on T^{-1}, predicted by this very simplified model, is quite well fulfilled here (Figure 8). The slope of the dependence gives the reasonable value ℓ = 13 Å. A quantum-chemical estimation leads to the quite close value ℓ = 15 Å for the length of the 6CB molecule.

Figure 7 shows that the transition from the isotropic to the nematic phase manifests itself not only by a jump in the relaxation time τ_1, but also by a considerable increase of the activation energy. Simultaneously, the activation energy for the viscosity is practically equal for both phases. This reflects the contribution of the nematic potential to the dynamics of nematogenic molecule.

On the basis of the values of the relaxation times in the nematic and isotropic phases for the process corresponding to the molecular rotation around the short axis one can determine the orientational order parameter of 6CB and the height of the nematic potential as a function of temperature using the theory proposed by Martin et al. [19, 20]. According to this theory, the relaxation time in the presence of the nematic potential (τ_1) is longer than that in the absence of the nematic potential (τ_0) by a factor

$$g^* = \frac{\tau_1(q \neq 0)}{\tau_0(q = 0)}, \tag{13}$$

called the retardation factor. Here q is the height of the nematic potential barrier and τ_0 is the value of the relaxation time extrapolated from the $\tau_1(T)$ dependence in the isotropic phase to a given temperature in the nematic phase.

According to the Maier-Saupe mean field theory [21], the nematic potential can be presented in the form

$$U(\Theta) = q \cdot P_2(\cos \Theta), \tag{14}$$

where $P_2(\cos \theta)$ is the second Legendre polynomial and Θ the angle between the long molecular axis and the director $\boldsymbol{n}$.

The long-range orientational order is defined as the averaged second Legendre polynomial

$$S = \langle P_2(\cos(\Theta)) \rangle = \left\langle \frac{3}{2} \cdot \cos^2 \Theta - \frac{1}{2} \right\rangle = \frac{\int_0^{\pi/2} \left(\frac{3}{2} \cos^2 \Theta - \frac{1}{2} \right) \cdot f(\Theta) \cdot \sin \Theta \, d\Theta}{\int_0^{\pi/2} f(\Theta) \cdot \sin \Theta \, d\Theta}, \quad (15)$$

were the angular brackets mean averaging over the all possible positions of the molecules in time and space. Here $f(\Theta)$ is the undisturbed distribution function of the nematic order and can be presented in the form [19, 20]

$$f(\Theta) = f(0) \exp\left(-\frac{q}{kT} \sin^2 \Theta \right). \quad (16)$$

On the basis of the retardation factor g^*, the height of the potential barrier can be determined using the method proposed by Martin et al. [19]. The values of g^* and q for 6CB at various temperatures are gathered in Table 1. The temperature dependence of the order parameter S, calculated from (15) and (16), is presented in Figure 1. As can be seen, the $S(T)$ resulting from the temperature dependence of the dielectric ralaxation time corresponding to the molecular rotation around the short axis, is very close to the $S(T)$ dependences obtained with other, mainly spectroscopic methods.

Table 1. Retardation factor g^*, height of the potential barrier q for rotation around molecular short axis and nematic order parameters S for 6CB.

T/°C	g^*	q		S
		eV	kJ/mol	
19.4	4.79	0.081	7.78	0.46
20.4	4.67	0.080	7.69	0.46
21.4	4.34	0.077	7.47	0.44
22.4	4.05	0.074	7.13	0.42
23.4	3.78	0.071	6.84	0.41
24.4	3.52	0.068	6.55	0.39
25.4	3.26	0.063	6.08	0.36
26.4	3.01	0.061	5.85	0.35
27.4	2.73	0.058	5.62	0.33
27.9	2.58	0.056	5.38	0.32
28.4	2.41	0.054	5.20	0.31
28.6	2.36	0.051	4.95	0.29
28.8	2.31	0.048	4.64	0.27
28.9	2.09	0.044	4.27	0.25
29.0	1.99	0.042	4.02	0.23

Acknowledgement

This work was supported by the Polish Research Project No 2P03B 032 18 coordinated by the Committee for Scientific Research (KBN).

[1] W. D. de Jeu, Physical Properties of Liquid Crystalline Materials, ed. G. W. Gray, Gordon and Breach Sci. Publ., 1980.
[2] H. Kresse, Advances in Liquid Crystals, ed. G. H. Brown, Vol. 6, Academic Press, New York 1983, p. 109.
[3] S. Urban and A. Würflinger, Advances in Chemical Physics, ed. I. Prigogine and S. A. Rice, Vol. 98, John Wiley & Sons, New York 1997, p. 143.
[4] W. Maier and G. Meier, Z. Naturforsch. **16a**, 262 (1961).
[5] J. Jadżyn, S. Czerkas, G. Czechowski, and A. Burczyk, Liq. Cryst. **26,** 437 (1999).
[6] P. G. de Gennes and J. Prost, The Physics of Liquid Crystals, 2nd edition, Clarendon Press, Oxford 1993.
[7] C. J. F. Böttcher and P. Bordewijk, Theory of Electric Polarization, vol. II, Elsevier Scientific, Amsterdam 1978.
[8] J. Jadżyn, G. Czechowski, R. Douali, and C. Legrand, Liq. Cryst. **26,** 1591 (1999).
[9] D. Bauman, Mol. Cryst. Liq. Cryst. **172,** 41 (1989).
[10] P. P. Karat and N. V. Madhusudana, Mol. Cryst. Liq. Cryst. **36,** 51 (1976).
[11] H. Moryson, D. Bauman, and J. Jadżyn, Mol. Cryst. Liq. Cryst. **250,** 63 (1994).
[12] L. Onsager, J. Amer. Chem. Soc. **58,** 1486 (1936).
[13] A. Buka and W. H. de Jeu, J. Phys. Paris **43,** 361 (1982).
[14] D. A. Dunmur, M. R. Manterfield, W. H. Miller, and J. K. Dunleavy, Mol. Cryst. Liq. Cryst **45,** 127 (1978).
[15] P. Kędziora and J. Jadżyn, Mol. Cryst. Liq. Cryst. **192,** 31 (1990).
[16] S. Urban, Z. Naturforsch. **50a**, 826 (1995).
[17] K. S. Cole and R. H. Cole, J. Chem. Phys. **9,** 341 (1949).
[18] Mięsowicz, Nature London **136,** 261 (1935); **158,** 27 (1946).
[19] A. J. Martin, G. Meier, and A. Saupe, Symp. Faraday Soc. **5,** 119 (1971).
[20] G. Meier and A. Saupe, Liquid Crystals, Gordon and Breach Publishers, 1967, pp. 195–205.
[21] W. Maier and A. Saupe. Z. Naturforsch. **14a,** 882 (1960); **15a,** 287 (1960).